

# NUMERICAL ANALYSIS ON RIB-TUBES OF SEAWATER OPEN RACK VAPORIZER WITH THE SPOILER LEVER

## Su Houde

College of Petrochemical Engineering, Lanzhou University of Technology, Lanzhou, Gansu, China  
Gansu Lanpec Technologies Co. Ltd. , Lanzhou, Gansu, China

## Yu Shurong

College of Petrochemical Engineering, Lanzhou University of Technology, Lanzhou, Gansu, China

## Fan Jianling,

Shanghai University of Engineering Science, Shanghai, China  
School of Energy and Power Engineering, Lanzhou University of Technology, Lanzhou, Gansu, China

## Wei Xing

Gansu Lanpec Technologies Co. Ltd. , Lanzhou, Gansu, China

## ABSTRACT

*In order to explore a more reasonable structure and operating parameter, guide the design and improve the gasification of seawater Open Rack Vaporizer (ORV), Research on the rules of seawater that flows and heat transfer in the ORV tube was studied in this paper. By simplifying the model, heat transfer tube model with spoiler lever was obtained and simulated, the distribution of temperature field, gas ratio, velocity field and press field in rib tube were analyzed, and different inlet velocity of LNG, roughness of the tube wall both effected on the overall gasification, the results shows that the actual gasification efficiency from heat transfer tube is higher than normal, small difference of gas ratio outlet, velocity and temperature are both lower, LNG could be easier gasified at operating temperature between  $-162^{\circ}\text{C}\sim+3^{\circ}\text{C}$  than that between  $-162^{\circ}\text{C}\sim+0^{\circ}\text{C}$ .*

**Keywords:** The spoiler lever; Open Rack Vaporizer(ORV); Rib-tubes; Numerical simulation

## INTRODUCTION

Liquefied natural gas (LNG) -a kind of clean energy, has been developed and utilized by more and more people. At present, the domestic product of LNG is mostly air-heated vaporizer and heat water-bath vaporizer. During the research of laboratory studies and numerical simulation, domestic and foreign scholars have done a lot of work to the traditional baffle heat exchanger[1,2,3]. They have proposed the conception of porous volume rate, surface permeability, distributing resistance and heat-source distribute, and continuous improvement of the calculation model can calculate its flow and heat transfer process more accurately, analyze the

influential parameters and performance parameters. Besides, a new type of heat exchanger structure has been proposed[4]. While there are few studies about such efficient vaporizer as seawater open rack vaporizer.

Research on rib-tubes of seawater open rack vaporizer with spoiler lever is on the basis of deepening the investigation and digestion. Study the rules of seawater that flows and heat transfer in the ORV tube through the methods of combining theoretical analysis and numerical simulation to explore a more reasonable structure and operation parameters, that can provide references for practical engineering application, guide the design and improve the gasification of seawater Open Rack Vaporizer (ORV).

## VAPORIZER STRUCTURE AND WORKING PRINCIPLE

### VAPORIZER STRUCTURE

Open Rack Vaporizer (ORV) is a kind of heat exchanger using seawater as heat source. Structure diagram as shown in Fig.1[5].

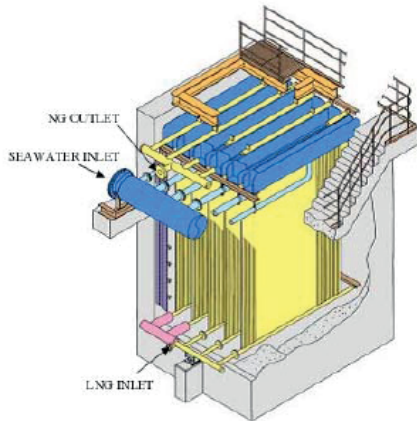


Fig. 1. Structural diagram of seawater ORV

### WORKING PRINCIPLE

Open Rack Vaporizer (ORV) is generally fixed with aluminum alloy holders. The basic cell of ORV is tube. There are several heat-exchange tube forming a tabular arrangement, both ends of which welded to the gas/liquid collector tubes to form a tubesheet, then these tubesheets constitute the vaporizer [6]. LNG flows into from the bottom pipe with a vertical upward mobility in the bundle, then seawater transfers the heat to LNG to make it gasification. There is a spray device on top of the ORV, which let seawater spray from top to bottom. After entering through the upper distribution, seawater flows down as film shape along the tube, and have LNG heated and gasified[7,8,9]. Working principle as show in Fig.2.

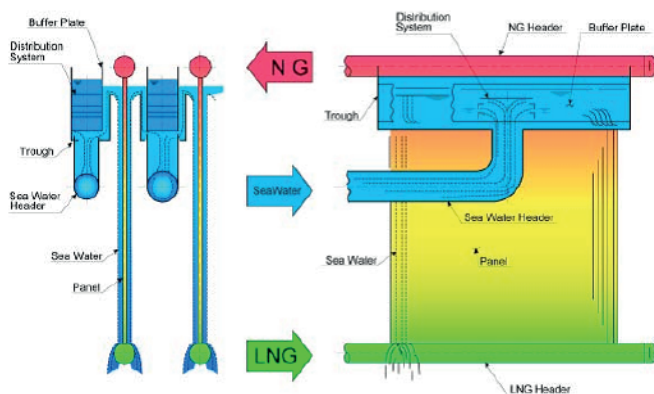


Fig. 2. Schematic diagram of seawater ORV

As Open Rack Vaporizer (ORV) has no moving parts and few instrument elements, switch of which can be remote controlled, and ORV can be hang on the scaffold, all these features make it easier to maintain. As long as altering the seawater flowing to the spray system and LNG through the tubes, the alteration of the operation loads can be easier. The ORV is consist of several independents, that can isolate parts of the bundle to reduce the loads[10].

## MODEL ESTABLISHING AND NUMERICAL ANALYSIS

### Parameters and Meshing of the Pump model

In actual manufacturing, the rib-tubes are generally with baffle rods, the baffle rods inserted into the tube is an effective way to enhance the heat transfer of fluids. This structure has several advantages such as simple structure, stable performance, easy installing and removing[11,12]. So establishing a rib-tube model with the baffle rods can simulate the work situation more actually.

Basic model structure of the baffle rods as shown in Fig.3. Crossing windings, whose thickness "b" is 1.2 mm. Length of the section crossing turning around 360° is 300 mm, and total length is 6000 mm, i.e. the length of the heat-exchange tube.

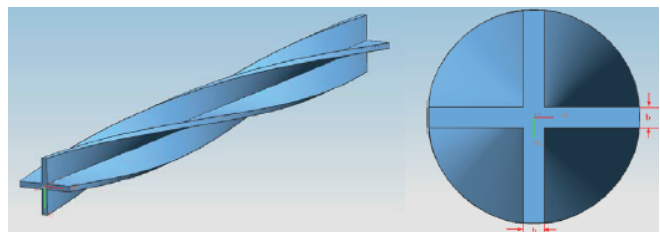
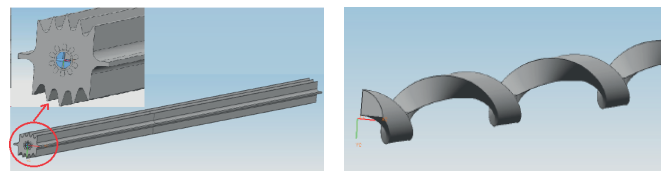


Fig. 3. The basic structure of the baffle rods

Using UG software to establish the model of flow field for the tube with baffle rods, corresponding to the real fitting length, tube side direction is "Z"axis. Fig.4(a) shows the UG model of flow field for the tube with baffle rods; Fig.4(b) shows the flow shape of the inner tube with inserter baffle rods when liquid passing by.

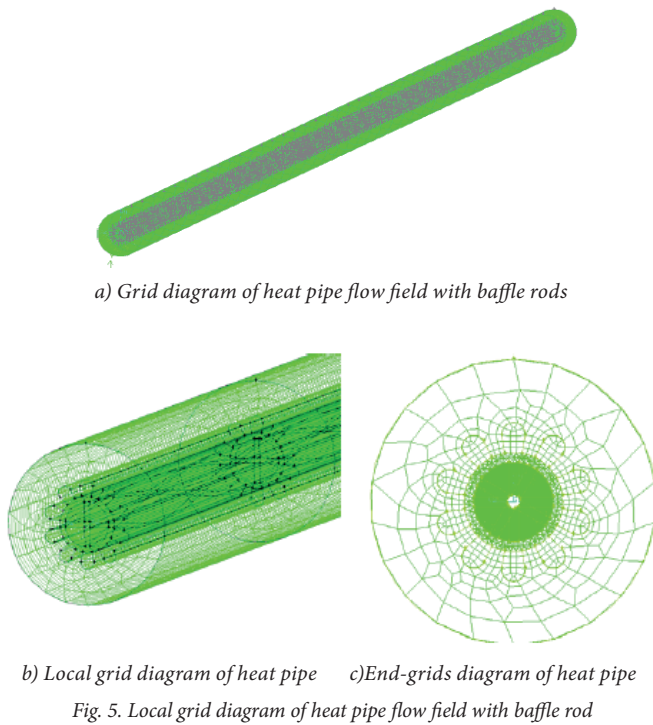


a) Calculation model of heat pipe flow field with baffle rod b) Model diagram of 1/4 the inner tube with baffle rod

Fig. 4. Calculation model of heat pipe flow field with baffle rod

Increased baffle rods cause pipe flow field to be rather complex, so non-structural tetrahedral meshing is adopted

for this project. Calculation results without baffle rods show that temperature distribution of the outer wall changes a little. In this case, irregular shape of the outer wall can be simplified to cylindrical surface in same diameter, that out-wall meshing can be generated by COPPER which ensure the grid quality and reduce the total number of grids. The rest of the inner grids are generated by the way of TGrid with a total number of 3699320. Fig.5(a) and Fig.5(b) shows the grids diagram of heat pipe with baffle rods; Fig.5(c) shows the end-grids diagram of heat pipe with baffle rods.



### Numerical method

In the heat pipe of the seawater open rack vaporizer, mixture model is selected for the gas-liquid 2-phases flow processes, and the calculation equation is as follows:

Continuity equation:

$$\frac{\partial}{\partial t}(\rho m) + \nabla \cdot (\rho_m \bar{v}_m) = \dot{m} \quad (1)$$

“ $\dot{m}$ ” means the mass transfer of user defined mass source;  $\bar{v}_m$ ,  $\rho_m$  describe the average velocity and mixture density of the mass respectively, can be required by formula (2)

$$\bar{v}_m = \frac{\sum_{k=1}^n a_k \rho_k \bar{v}_k}{\rho_m}, \rho_m = \sum_{k=1}^n a_k \rho_k / m \quad (2)$$

Here,  $a_k$  is volume fraction of the “k” phase;

Momentum Equation:

$$\begin{aligned} \frac{\partial}{\partial t}(\rho m) + \nabla \cdot (\rho_m \bar{v}_m) = & \\ -\nabla p + \nabla \cdot [u_m (\nabla \bar{v}_m + \nabla \bar{v}_m^T)] & \\ + \rho_m \bar{g} + \bar{F} + \nabla \cdot (\sum_{k=1}^n a_k \rho_k \overline{v_{dr,k} v_{dr,k}}) & \end{aligned} \quad (3)$$

Here, “n” means the phase,  $\bar{F}$  means the volume force,  $u_m$  means the mixed viscosity

Energy Equation:

$$\begin{aligned} \frac{\partial}{\partial t} \sum_{k=1}^n (a_k \rho_k E_k) + \nabla \cdot \sum_{k=1}^n (a_k \bar{v}_m (\rho_k E_k + p)) & \\ = \nabla \cdot (k_{eff} \nabla T) + S_E & \end{aligned} \quad (4)$$

Here,  $k_{eff}$  means the effective thermal conductivity, first item of the left side of the equation represents the energy transfer due to conductivity.  $S_E$  contains all volume heat sources.

As the simulation involves phase transition, flow and conductivity. Firstly, solving the adiabatic flow, i.e. iteration of no coupling energy equation, and take this convergent flow field into the energy equation for the solution, finally you will get the exact solution after the computed convergence. Residual of the convergence criteria is less than  $10^{-3}$ , while residual of the energy equation among which is less than  $10^{-6}$ , that it can ensure the stability of outlet’s velocity and temperature.

## SIMULATION RESULTS AND ANALYSIS

Analysis for operation temperature:  $-162^{\circ}\text{C} \sim 0^{\circ}\text{C}$

Through the numerical simulation of the heat pipe model with baffle rods and heat transfer, it can be obtained the velocity field distribution, temperature field distribution, pressure field distribution and LNG outlet parameters, LNG outlet velocity is 2.125562m/s, and the average temperature at the outlet is  $T = 266.8662\text{K}$ . Actual flow state and heat transfer can be easily observed from these calculation results.

Temperature field distribution rules

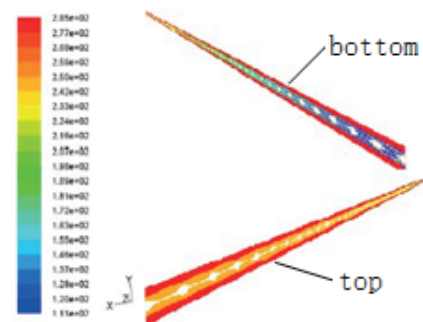


Fig. 6. Temperature distribution in actually the pipe symmetry plane

Fig.6 shows the temperature field cloud diagram. It can be seen from the diagram that with the temperature of LNG along the tube side rising continuously, the increased baffle rods is equivalent to increase the flow path of the fluid in the heat pipe, as the LNG endothermic process increased, the gasification process would be enhanced correspondingly. It can also be seen from Fig.6 that the temperature has no obvious gradient changes of rather a long tube at the top, indicating that the heat has achieved a balance provided by the out wall heat source, temperature increase indicating that two-phase fluids have generated, low-temperature area stating liquid abounds, higher temperature area stating gas abounds

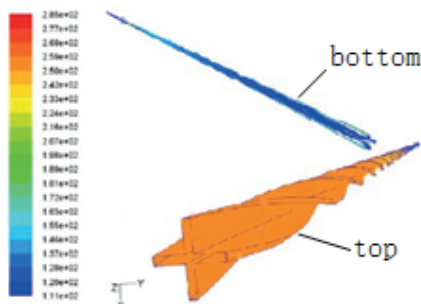


Fig.7. Temperature contours of spoiler lever wall

Fig. 7 shows the temperature distribution cloud diagram of the baffle rods wall. Seeing from the diagram, the bottom spoiler surface along radial direction has temperature gradient, which increases gradually along the tube side. The closer to the top of the outlet, temperature distribution presents more uniformly, and top baffle rods has no obvious gradient along the radial direction.

### Study of gas phase composition distribution

In order to clearly reflect the gasification process of the actual heat pipe model, multiple crossing sections have been intercepted to observe each crossing section's gas content distribution changes. As shown in Fig.8(a)~(f)

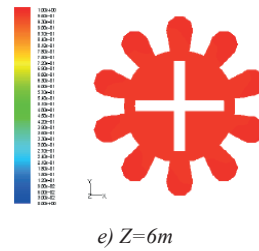
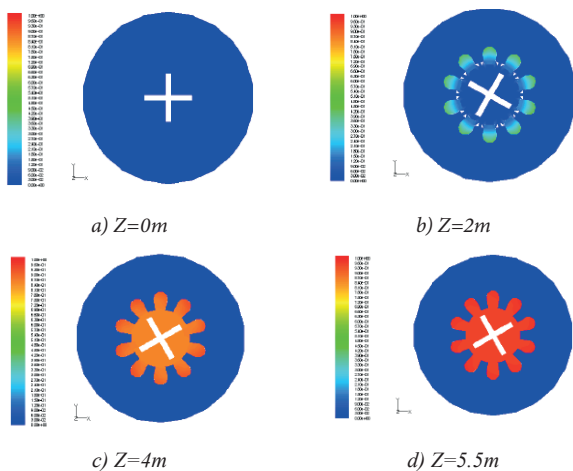


Fig. 8. LNG volume fraction contours

Seeing from Fig.8, gasification process of LNG in the annular space is faster than that in the inner tube. In evaporation section(below 2.5m), the gasification process doesn't show an obvious reinforcement, the slow gasification mainly because the fluid disturbance caused by the baffle rods improved the inner wall heat transfer coefficient, heat incoming from outer wall being absorbed by the LNG of inner tube, which leads to a slow heat absorption of LNG in the annular space. After entering into the heating section, two parts of fluids mixes, and with the effects of baffle rods' disturbance, mixing degree hightens and gas content ratio distributes uniformly, gas content ratio at the outlet is higher than that of no-baffle rods model, that can reach to 0.99984, so it can be considered that gas at the actual heat pipe outlet is of LNG.

### Velocity contours regulation

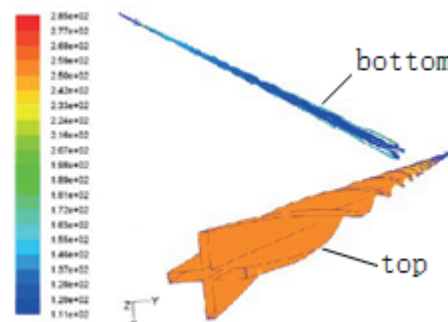


Fig. 9. Velocity contours of actual heat transfer tube symmetry plane

Fig.9 shows the velocity contours of actual heat transfer tube symmetry plane. Seeing from this plane, the actual velocity distribution inside the annular space of actual pipe is basically the same with that inside the annular space of non-baffle rods model, the only difference is the velocity distribution in the inner tube, effects of baffle rods brings a radial velocity of the fluid in the inner tube, which would enhance the flushing effects of the inner wall and improve the heat transfer coefficient.

### Pressure contours regulation

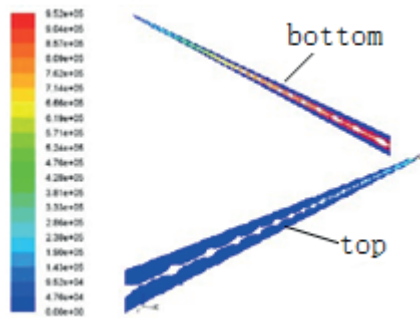


Fig.10. Pressure contours of actual heat transfer tube symmetry plane

Fig.10 shows the pressure contours of actual heat transfer tube symmetry plane. It can be seen from Fig.10 that pressure contours is basically the same with non-baffle rods model. As the pressure decreases gradually, the distribution shows uniformly. As the actual heat pipe model added with spoiler parts, fluid losses increase.

### ANALYSIS FOR OPERATION TEMPERATURE: $-162^{\circ}\text{C}\sim 3^{\circ}\text{C}$

#### Temperature field distribution rules

Fig.11 shows temperature distribution in actually the pipe symmetry plane, Fig.12 shows temperature distribution in turbulence pole wall.

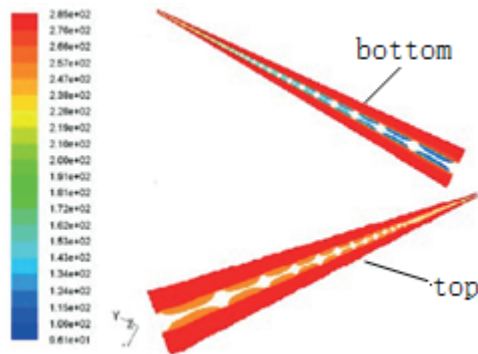


Fig. 11. Temperature distribution in actually the pipe symmetry plane

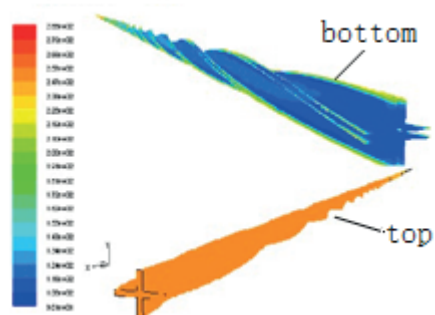


Fig. 12. Temperature distribution in turbulence pole wall

Seen from Fig.11 and Fig.12, combined with Fig.6 and Fig.7, temperature distribution of the actual pipe symmetry plane and that of the baffle rods surface contrast with the temperature of  $-162^{\circ}\text{C}\sim 0^{\circ}\text{C}$ , the variation tendency reach to a consistency. It has a larger temperature range for the operation temperature of  $-162^{\circ}\text{C}\sim 3^{\circ}\text{C}$  than  $-162^{\circ}\text{C}\sim 0^{\circ}\text{C}$ , with a same maximum, the minimum operation temperature of  $-162^{\circ}\text{C}\sim 3^{\circ}\text{C}$  is lower than that of  $-162^{\circ}\text{C}\sim 0^{\circ}\text{C}$ .

#### Study for gas phase composition distribution

Fig.13 shows the gas fraction in the pipe cross section.

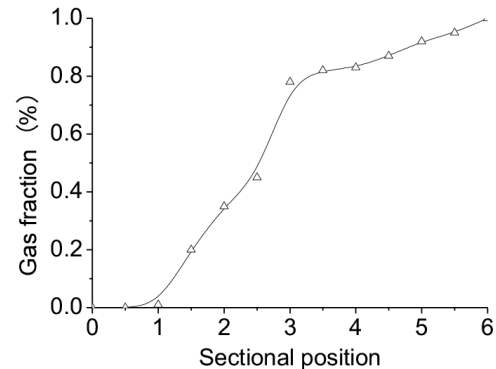


Fig.13. Gas fraction in the pipe cross section

Seen from Fig.13, gas fraction, which increases along the pipe cross section, changes slowly at the top and bottom of the heat pipe, and increases sharply in the middle section, these mainly because the baffle rods' reinforcing and mixing effects make the gasification speed up and gas fraction increase after passing through the heat pipe.

#### Velocity distribution in actually the pipe

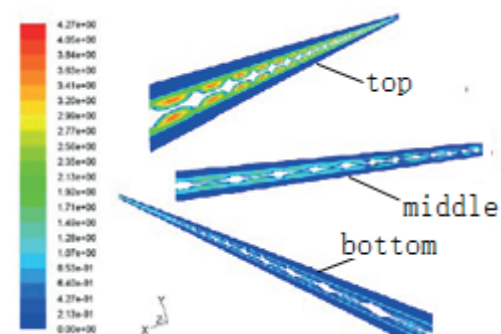


Fig. 14. Velocity distribution in actually the pipe

Fig.14 shows the diagram of the velocity distribution in actually the pipe. Combined with Fig. 9, It has a larger velocity range for the operation temperature of  $-162^{\circ}\text{C}\sim 3^{\circ}\text{C}$  than  $-162^{\circ}\text{C}\sim 0^{\circ}\text{C}$ , while the velocity variation is nearly the same at all positions, which indicating that changes of temperature only have effects on velocity's value instead of distribution.

## Study for pressure distribution in actually the pipe top symmetry

Fig.15 shows the pressure distribution in actually the pipe top symmetry.

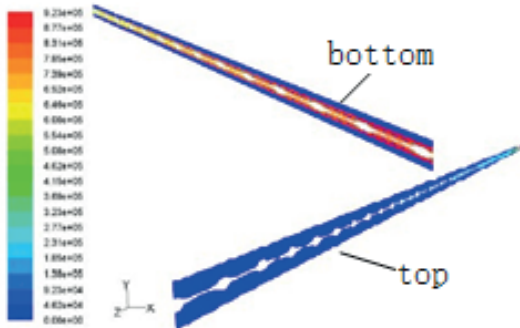


Fig. 15. Pressure distribution in actually the pipe top symmetry

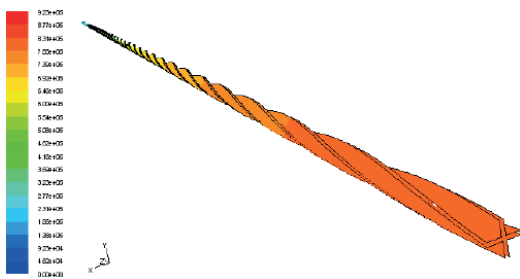


Fig. 16. Pressure distribution in turbulence pole

Compared with the calculated point at the former boundary conditions (operation temperature:  $-162^{\circ}\text{C}\sim 0^{\circ}\text{C}$ ), no obvious changes appear, the only outlet temperature and velocity changes are all within a reasonable range.

## ANALYSIS OF FACTORS INFLUENCING THE GAS FRACTION

### EFFECTS OF GAS FRACTION AT THE INLET

Under the condition of unchanging the pipe model, numerical stimulations were respectively taken for the inlet velocity of 0.3m/s, 0.5m/s, 0.76447m/s, 0.9m/s, the required LNG gas fraction distribution in actual the pipe each section under different velocity is as shown in Fig.17.

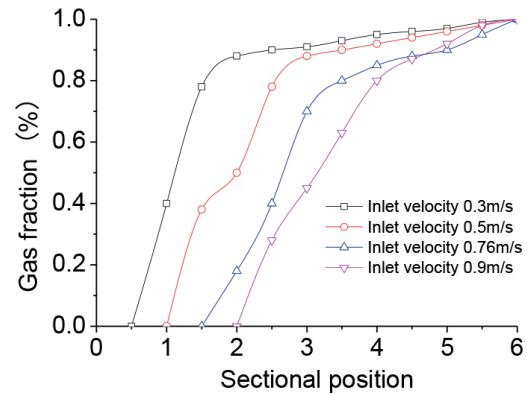


Fig. 17. LNG gas fraction distribution in actual the pipe each section under different velocity

Seen from Fig.17, the lower of the LNG inlet velocity, the fuller of the LNG gasification process, this mainly because as the drop of inlet velocity, the heating time of LNG in tube is relatively longer, and the gasification process is fuller. Compared with the gas fraction at the height of 2m section, gasification degree of the gas fraction has obvious discrepancy under different flow rate. At the speed of 0.3m/s and height of 2m, the gas fraction can reach to nearly 0.9. While at the inlet speed of 0.9m/s, the gas fraction just reach to 0.2 at the same position, so the inlet velocity has a great influence over the whole gasification for the baffle-rods model.

### EFFECTS OF INNER WALL ROUGHNESS ON GAS FRACTION

If other conditions are the same, considering the effects of inner wall roughness on gas fraction, respective calculation at the condition of these roughness:10(Ra 0.2), 9(Ra 0.4), 8(Ra 0.8), 7(Ra 1.6) give the gas fraction distribution in actual the pipe each section under different roughness as shown in Fig.18.

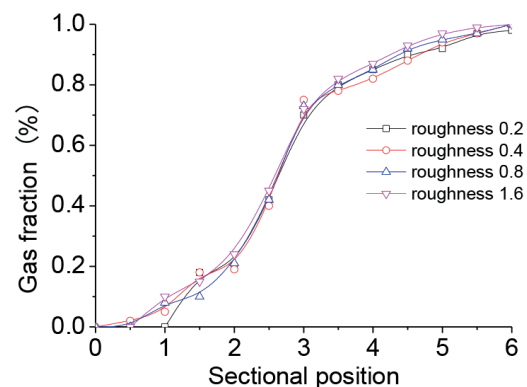


Fig. 18. LNG gas fraction distribution in actual the pipe each section under different roughness

Seen from Fig.18, the whole gasification of the actual heat pipe is basically the same for different roughness, increasing along the tube side. In evaporation zone of the heat pipe(before 2.5m), gas fraction varied obviously as the

variation of roughness, after then which varied slowly as the variation of roughness. Since at the tube side before 2.5m, with the inner pipe roughness increased, the tube wall's effects on the fluids increased, gas fraction of each cross section increased and the gasification quicken. And because of the increased baffle rods of the actual pipe model, the flow mixing and gasification increase quickly. At the tube side after 2.5m, gas fraction appears an obvious variation when  $Ra=1.6$ , but the amplification if not great, since the gas fraction has already been closer to 100%.

### EFFECTS OF BAFFLE RODS ON GAS FRACTION

Fig.19 shows the void fraction distribution of heat pipe cross section.

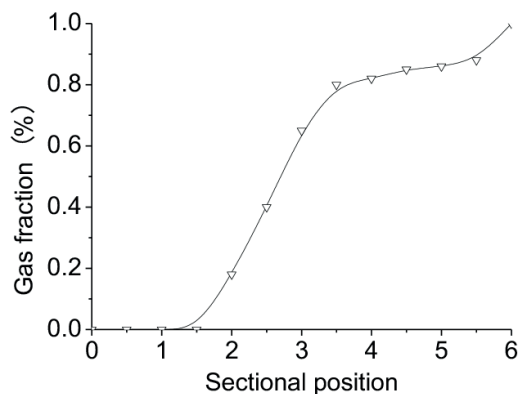


Fig.19. Void fraction distribution of heat pipe cross-section

Seen from Fig.19, the whole gasification process is increasing gradually along the tube side, with the rising of temperature, gasification and gas fraction is increasing gradually. From inlet to the height of 1.5m, gas fraction is 0, because the low temperature LNG endothermic process needs a certain period of time, only reach to the phase transition, can gasification be processed properly and can have LNG. It would appeared a period with gas fraction sharply rising between 2m and 3m, that indicating the fluids mixing even more sharply at the connection of the actual pipe evaporation and heating area, the gasification process and the whole gasification increased.

### CONCLUSION

(1) Under the same boundary conditions, the gasification efficiency is higher for the baffle-rods heat pipe, gas content at the outlet differs a little, velocity and temperature are both lower[13].

(2) If other conditions are the same, gas fraction varies a little alone the tube side, with the increase of the inner wall roughness, gasification of the model with baffle-rods that increases in the evaporation zone along the tube side and increases slightly at the heating section.

(3) Outlet velocity at the operation temperature:  $-162^{\circ}\text{C} \sim +3^{\circ}\text{C}$  is higher than that at the operation temperature:

$-162^{\circ}\text{C} \sim 0^{\circ}\text{C}$  by 7.233%, average temperature at the outlet increased 0.59855%, gas fraction reaches to 0.999913, these indicates a total gasification.

### BIBLIOGRAPHY

1. S. Prasanth Kumar, B.V.S.S.S. Prasad, G. Venkatarathnam, K. Ramamurthi: Influence of Surface Evaporation on Stratification in Liquid Hydrogen Tanks of Different Aspect Ratios. *Int. J. Hydro Energy*, 32, 1954,2007.
2. B.Zhang,W.Q.Wu: Effert of Environmental Temperature and Wind Velocity on Underwater LNG Vessel Leakage. *J. Harbin Eng. Univ.*, 30(8), 855,2009.
3. Y.D.Chen, X.D.Chen: A Technical Analysis of Heat Exchangers in LNG Plants and Terminals. *Nat Gas Ind*, 30(1), 96,2010.
4. D.A Kesten, Clean Fuel-LNG,.Messer SAIC, 5(08),27,2000.
5. C.H.Son, S.J. Park. An Experiment Study on Heat Transfer and Pressure Drop Characteristics of Carbon Dioxide During Gas Cooling Process in a Horizontal Tube.*Int. J. Refrigeration*,29 (1),539,2006.
6. L.R.Wei, Y.Q.Xia, D.P.Wang: Light Hydrocarbons Separation Process in Refinery by Using LNG Cold Energy. *Acta Petrol Sin(Petrol Proc Sec)*, 31(6), 1317,2015.
7. S.W.Qian: Fluid Mechanics and Heat Transfer of Heat Exchanger Tubes. China Petrochemical Press, Beijing, 2002.
8. P.Xie, Zh.W.Xian: SPECIAL SUBJECT: Liquefied Natural Gas(LNG) Technology. *Nat Gas Oil*, 23 (02), 6,2005.
9. S.Chen, X.Z.Zhang: Energy-saving Operation of ORV under Low Seawater Temperatures at LNG Terminals, *Nat Gas Ind*, 36(5), 106,2016.
10. W.Sh.Tao: Numerical Heat Transfer. Xi'an Jiaotong University Press, Xi'an, 2002
11. J.V.Leyendekkers, Q.Ch.Cui, W.M.Dai: Seawater Thermodynamics. China Ocean Press, Beijing,1981
12. K.Zhang, C.L.Han, J.J.Ren, Y.H.Zhou, M.S.Bi: Numerical Simulation on Heat Transfer of Supercritical LNG in Coil Tubes of Submerged Combustion Vaporizer, *J Chem Ind Eng.(China)*, 66(12), 4788,2015.
13. Z. H. Hu, T. K. Huang, L. Y. Zhang, M. Yang: Numerical Simulation of Coupled Heat Transfer for LNG Pipeline, *J Chem Ind Eng.(China)*, 66(S2), 206,2015.

**CONTACT WITH AUTHOR**

**Houde Su**

*e-mail: suhoude@lanpec.com*

tel.: 13919158139

College of Petrochemical Engineering

Lanzhou University of Technology

Lanzhou, Gansu, 730050

**CHINA**